New Phytologist

Research

Comparative transcriptome analysis of cadmium responses in *Solanum nigrum* and *Solanum torvum*

Jin Xu[1,2], Jianhang Sun[1], Liguo Du[1] and Xiaojing Liu[1,2]

[1]Key Laboratory of Agricultural Water Resources, Center for Agricultural Resources Research, Institute of Genetics and Developmental Biology, Chinese Academy of Sciences, 286 Huaizhong RD, Shijiazhuang 050021, China; [2]Hebei Province Engineering Laboratory for Plant Breeding and Germplasm Enhancement of Stress-Tolerant Plants, 286 Huaizhong RD, Shijiazhuang 050021, China

Author for correspondence:
Jin Xu
Tel: +86 311 85871745
Email: xujin@sjziam.ac.cn

Received: *29 February 2012*
Accepted: *3 June 2012*

New Phytologist (2012)
doi: 10.1111/j.1469-8137.2012.04235.x

Key words: accumulation, cadmium (Cd), iron (Fe), *Solanum nigrum*, *Solanum torvum*, tolerance, transcriptome analysis.

Summary

- *Solanum nigrum* is a cadmium (Cd) accumulator, whereas *Solanum torvum* is a low Cd-accumulating plant. The molecular mechanisms that are responsible for differential cadmium (Cd) accumulation in the two *Solanum* species are poorly understood.
- Here, grafting experiments confirmed that increased Cd loading into the root xylem was responsible for the differential Cd accumulation in the two *Solanum* species. An iron (Fe) supply assay indicated that low Fe accumulation in *S. torvum* leaves is related to its Cd sensitivity.
- Transcriptome analyses revealed higher expression of the genes that encode several metal transporters as well as antioxidant-related genes, and several organic and amino acid biosynthesis/metabolism-related genes in Cd-treated *S. nigrum*. Our data also indicated that the different responsive mechanisms of the transporter genes to Fe deficiency might be responsible for differential uptake and redistribution of metals in the two *Solanum* species
- These results form a basis upon which to further explore the molecular mechanisms of Cd accumulation and tolerance, and provide an insight into novel strategies that can be used for phytoremediation and food safety.

Introduction

Cadmium (Cd) is one of the most toxic nonessential elements, and it has a strong inhibitory effect on plant growth and reproduction (Macek *et al.*, 2002). In leaves, concentrations of Cd that are higher than 5–10 μg g^{-1} DW are toxic to most plants (White & Brown, 2010; Lux *et al.*, 2011). By contrast, some species can hyperaccumulate Cd to concentrations in excess of 100 μg g^{-1} DW in their leaves without showing any negative symptoms. Another strategy that allows plants to avoid Cd toxicity has emerged through natural evolution; some plants sequester Cd in their roots and prevent the translocation of Cd into the shoots, or remobilize Cd from shoots to roots by excluding Cd from leaves through the phloem (Chen *et al.*, 2006; Mendoza-Cózatl *et al.*, 2011). These plants are referred to as low Cd-accumulating plants (Yamaguchi *et al.*, 2010). The typical characteristics of hyperaccumulator plants include: the high efficient uptake of Cd in roots; xylem loading and transport from the roots to the shoots; and the capacity to effectively detoxify Cd. Many studies regarding the molecular mechanisms of Cd hyperaccumulation have been reported; however, the molecular mechanisms that are responsible for low Cd accumulation in plants are poorly understood (Yamaguchi *et al.*, 2010).

Cadmium is chemically similar to certain metal elements, including iron (Fe), zinc (Zn) and calcium (Ca), and, therefore, could displace these elements from metalloproteins (Clemens *et al.*, 1998; Cohen *et al.*, 1998; Verbruggen *et al.*, 2009). Cd toxicity can be attributed to its competition with essential metals, especially Fe, for metal-binding molecules (Schutzendubel & Polle, 2002). Cd enters plant cells through Fe, Ca and Zn transporters/channels (Wu *et al.*, 2012). Several studies have shown that Cd toxicity led to Fe deficiency in plants (Lombi *et al.*, 2002; Yoshihara *et al.*, 2006; Besson-Bard *et al.*, 2009). However, the molecular mechanism of Fe accumulation on Cd tolerance and accumulation is still not fully understood.

Solanum nigrum is a Cd accumulator that is widely grown in Asia, Europe, and America. In a pot-culture experiment, *S. nigrum* accumulated 125 μg Cd g^{-1} of leaf DW without showing any phytotoxic symptoms or visible growth reduction (Sun *et al.*, 2006). Most Cd hyperaccumulators grow slowly and have a low biomass; however, *S. nigrum* has a faster growth rate and higher biomass, and therefore *S. nigrum* shows more promise for use in phytoremediation (Wei *et al.*, 2004). *Solanum torvum* cv. Torubamubiga is a low Cd-accumulating plant. Arao *et al.* (2008) found that, although the Cd concentration in *S. torvum* shoots was lower than that found in *S. melongena*, there was no difference in the Cd concentration that was measured in the roots of *S. torvum* and *S. melongena*. Further studies indicated that although all of the root uptake, xylem loading, and sequestration are responsible for the Cd accumulation in plants, the low

loading rate of Cd into the xylem sap in the roots is the major contributor for the low Cd translocation to the above-ground parts of *S. torvum* (Mori *et al.*, 2009).

The distinct types of Cd accumulation in the two *Solanum* species make *Solanum* an ideal genus in which to compare the physiological and molecular mechanisms that are involved in differential Cd accumulation. In this study, we compare Cd tolerance and accumulation between the Cd accumulator *S. nigrum* and the low Cd accumulator *S. torvum*. We investigated the molecular mechanisms that are responsible for Cd tolerance and accumulation using a combination of physiological and transcriptome analyses. These results form a basis upon which to further explore the molecular mechanisms of Cd accumulation and tolerance, and provide an insight into novel strategies that can be used for phytoremediation and food safety.

Materials and Methods

Plant materials and growth conditions

The seeds of *S. nigrum* L. and *S. torvum* Sw. were kindly provided by the Germplasm Bank of Wild Species in Southwest China. To obtain seedlings, the seeds were sown under sterile conditions in Petri dishes that contained MS medium (Murashige & Skoog, 1962) and were solidified with 0.8% (w/v) agar (Sigma). Seven-day-old seedlings were transferred into Hoagland solution (Hoagland & Arnon, 1950) and were grown in a sterilized, pathogen-free glasshouse. The cultures were maintained at 22–25°C under a 16 h photoperiod. The treatment with $CdCl_2$ and/or 50 μM Fe-EDDHA (ethylendiamine-di (o-hydroxyphenylacetic) acid) was applied to 4-wk-old seedlings that were grown in Hoagland solution. The culture solution was replaced every 3 d.

Phenotypic analysis

Four-week-old plants that were grown in Hoagland solution were treated with $CdCl_2$ (20, 50, or 100 μM) for 7 d. The relative root growth was calculated as the root length grown in the presence of Cd divided by the mean root length under control conditions as described by Freeman *et al.* (2010). Nine replicate plants were measured for each plant species and treatment.

Inductively coupled plasma mass spectroscopy (ICP-MS) analysis

Four-week-old plants that were grown in Hoagland solution were treated with 50 μM $CdCl_2$ for 12 h, or 1, 3, or 5 d. The treated roots were immersed in a solution that contained 1 mM EDTA for 2 h and then thoroughly rinsed with distilled water. The samples were oven-dried at 75°C for 48 h. The dried plant tissues were ground and digested in concentrated nitric acid for 2–3 d at room temperature. The samples were then boiled for 1–2 h until they were completely digested. After adding 4 ml of Millipore-filtered deionized water and a brief centrifugation, the contents of Cd, Zn, Fe, Mn and Cu were determined using ICP-MS. Each experiment was repeated at least five times.

Measurement of Cd^{2+} flux with the scanning ion-selective electrode technique (SIET)

The net Cd^{2+} flux was measured noninvasively using SIET (BIO-001A; Younger USA Sci. & Tech. Corp., Beijing, China). SIET is a technique that specifically detects ion or molecule flow and velocity. Ion-selective microelectrodes with an external tip diameter of *c.* 3 μm were manufactured and silanized with tributylchlorosilane, and the tips were backfilled with a commercially available ionselective cocktail (Cd Ionophore I, 20909, Fluka, Switzerland). Previous study has proved that the Cd^{2+} electrode was highly discriminatory against other cations and demonstrated the utility of an ion-selective Cd^{2+} microelectrode as a research tool to study heavy-metal transport in biological systems (Piñeros *et al.*, 1998). The microelectrodes were calibrated in 50 and 500 μM Cd^{2+} before the flux measurement. Only the electrodes with Nernstian slopes > 25 mV per decade were used (Ma *et al.*, 2010). After exposure to 50 μM $CdCl_2$ for 24 h, the root segments were sampled for the Cd^{2+} flux measurement. The measuring solution contained 50 μM $CdCl_2$, 100 μM KCl, 20 μM $CaCl_2$, 20 μM $MgCl_2$, 500 μM NaCl, 100 μM Na_2SO_4 and 300 μM 2(N-morpholino) ethane sulfonic acid (MES), pH 5.7. SIET measures the concentration gradient of Cd^{2+} by means of a Cd^{2+}-specific microelectrode vibrated between two different detection points on the root surface at a distance of 1.5 μm. Ion flux data were subsequently calculated. The Cd^{2+} flux data were recorded for a period of 10–15 min. The flux data were obtained with the ASET software, which is part of the SIET system. The three-dimensional ionic fluxes were calculated using MageFlux (http://xuyue.net/mageflux). The negative values in the figure represent the cation influx or anion efflux and vice versa.

Grafting experiment

Grafting was performed in 3-wk-old plants, and this included reciprocal and self-grafting. In this experiment, the *S. torvum* plants were grafted onto *S. nigrum* (St/Sn) or *S. torvum* (St/St, self-grafting), and the *S. nigrum* plants were grafted onto *S. torvum* (Sn/St) or *S. nigrum* (Sn/Sn, self-grafting). After allowing the graft to establish for 2 wk, the plants were transferred to a fresh hydroponic medium containing 50 μM $CdCl_2$ for 24 h, and the subsequent determination of Cd accumulation in the scion shoots was performed as described earlier. At least six replicate plants were measured for each plant species and treatment.

Digital transcriptomics

Four-week-old *S. nigrum* and *S. torvum* plants were treated with 50 μM $CdCl_2$ for 24 h. The RNA was extracted from the roots of the control and the two treated *Solanum* species using TRIzol (Gibco/BRL, Life Technologies, Grand Island, NY, USA). The detailed experimental procedure and bioinformatics analysis for the digital gene expression (DGE) profiling are described in the Supporting Information (Methods S1 and Figs S3–S5).

Reverse transcription polymerase chain reaction (RT-PCR) analysis of gene expression

The plant sample preparation, RNA extraction and RNA quality and integrity check have already been described. For the semi-quantitative RT-PCR, we performed control reactions using the *18S rRNA* and *UBQ14* primers to ensure that an equal amount of RNA was used in each set of reactions. We optimized the cycle numbers to ensure that the amplification reaction was performed in the exponential phase. The transcriptome results were also verified using RT-quantitative PCR (RT-qPCR) according to the Minimum Information for Publication of Quantitative Real-Time PCR Experiments (MIQE) guidelines (Bustin *et al.*, 2009). The detailed experimental procedure for the RT-qPCR analysis is described in Methods S1.

Measurement of photosynthesis

The photosynthetic rate (*Pn*) was recorded on fully expanded leaves of the second youngest node at 0, 1, and 5 d separately after 50 μM $CdCl_2$ treatment using an intelligent portable photosynthesis system (LCpro+, ADC, UK). These observations were recorded on six to eight plants per treatment.

Detection of reactive oxygen species (ROS) concentrations

To measure the O_2^- content, the treated plant materials (0.5 g) were ground in liquid nitrogen. The obtained powder was suspended in 50 mM phosphate-buffered saline (PBS) buffer (pH 7.8). After centrifugation (15 min, 12 000 ***g***), the supernatant was used for O_2^- content measurements as previously described (Verma & Mishra, 2005).

For H_2O_2 content determination, the tissue powder was suspended in 100 mM PBS buffer (pH 7.8) that contained 1% (w/v) polyvinylpyrrolidone (PVP). After centrifugation (20 min, 12 000 ***g***), the supernatant was used for H_2O_2 content measurements as described by Verma & Mishra (2005).

Measurement of oxidative damage

The Cd-induced oxidative damage (membrane liquid peroxidation) was estimated by measuring the malondialdehyde (MDA) concentrations. Fresh plant tissues were homogenized in 0.1% (w/v) trichloroacetic acid (TCA) solution. After centrifugation (15 min, 12 000 ***g***), an aliquot of the supernatant was added to 0.5% thiobarbituric acid (TBA) in 20% TCA and heated at 90°C for 30 min. After cooling on ice, the mixture was centrifuged at 8000 ***g*** for 5 min. The absorbance was recorded at 532 and 600 nm. The MDA concentration was calculated from the difference between the absorbance values at 532 and 600 nm (Ben Amor *et al.*, 2005).

The degree of membrane integrity was also assessed by the percentage of electrolyte leakage. Leaves and roots were immersed in 10 ml of ddH_2O (double-distilled water) and incubated at 25°C for 2 h. The suspension medium was measured for the initial electrical conductivity (EC1). The samples were then boiled at 100°C for 15 min to release all the electrolytes, cooled and the final electrical conductivity (EC2) was measured. The electrolyte leakage was calculated using the formula $(EC1/EC2) \times 100\%$ (Wang *et al.*, 2008).

Statistical analysis

For each treatment, at least eight plants were analyzed; all the experiments were repeated at least three times. The results are presented as means ± SD. For statistical analysis, we used ANOVA and Tukey's test with the SPSS 16.0 software package (SPSS, Chicago, Illinois, USA). Differences between the treatments were tested by the least significant difference (LSD) test at a 0.05 probability level.

All sequence data for this study were archived at the National Center for Biotechnology Information's Short Read Archive (SRA) under accession no SRA053699.

Results

Cd tolerance assay

To compare the Cd tolerance in *S. nigrum* and *S. torvum*, 28-d-old plants were exposed to three Cd concentrations, 20, 50, and 100 μM, for 7 d. When the plants were grown without Cd, the roots of *S. nigrum* grew 1.14-fold longer than those of *S. torvum* (data not shown). Therefore, we used relative root growth to evaluate the Cd tolerance of the two species (Fig. 1a). At 20 μM Cd, the relative root growth of the two *Solanum* species was nearly identical. When the plants were exposed to 50 and 100 μM Cd, the root growth rate of *S. nigrum* was 1.34- and 1.27-fold higher, respectively, than that of *S. torvum*; these results indicated that *S. nigrum* is more tolerant to Cd stress than *S. torvum*. No obvious stress phenotype was observed in either of the plants after 7 d of 50 μM Cd treatment; however, 100 μM Cd led to visible leaf chlorosis and necrosis (data not shown). Therefore, we selected a Cd concentration of 50 μM for use in this study.

Cd uptake and accumulation

We measured the Cd content in both species. As shown in Fig. 1(b,c), the Cd accumulation in the plants increased with the duration of the treatment. After 1 d exposure to 50 μM $CdCl_2$, the Cd in the leaves reached a concentration that was *c.* 50% of the Cd accumulation level observed after 3–5 d. Compared with *S. torvum*, the Cd concentration that was observed in *S. nigrum* was threefold higher in the leaves and 1.2-fold higher in the roots. *S. nigrum* also showed a higher Cd leaf : root ratio than *S. torvum* (Fig. 1d). The low Cd leaf : root ratio and Cd concentrations in the *S. torvum* leaves indicated that *S. torvum* has a comparatively low Cd-accumulating capacity.

To compare the root Cd uptake in the two *Solanum* species, we used SIET to investigate the Cd^{2+} flux in the roots of *S. nigrum* and *S. torvum*. The $CdCl_2$ treatment caused a steady net Cd^{2+} influx at the region that was located 0–2900 μm from

New Phytologist

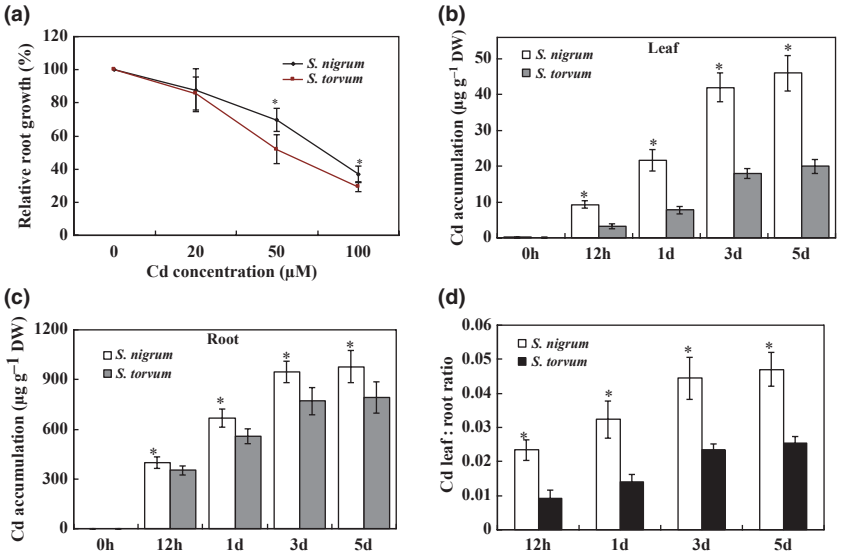

Fig. 1 (a) Relative root growth of *Solanum nigrum* and *Solanum torvum* plants that were exposed to Cd^{2+} for 7 d. The Cd content in the 4-wk-old (b) leaves, (c) roots, and (d) the Cd leaf : root ratios of the plants that were grown in Hoagland solution and treated with 50 μM $CdCl_2$. The asterisks indicate the values that were significantly different from those of *S. torvum* ($P < 0.05$). Error bars indicate ± SD.

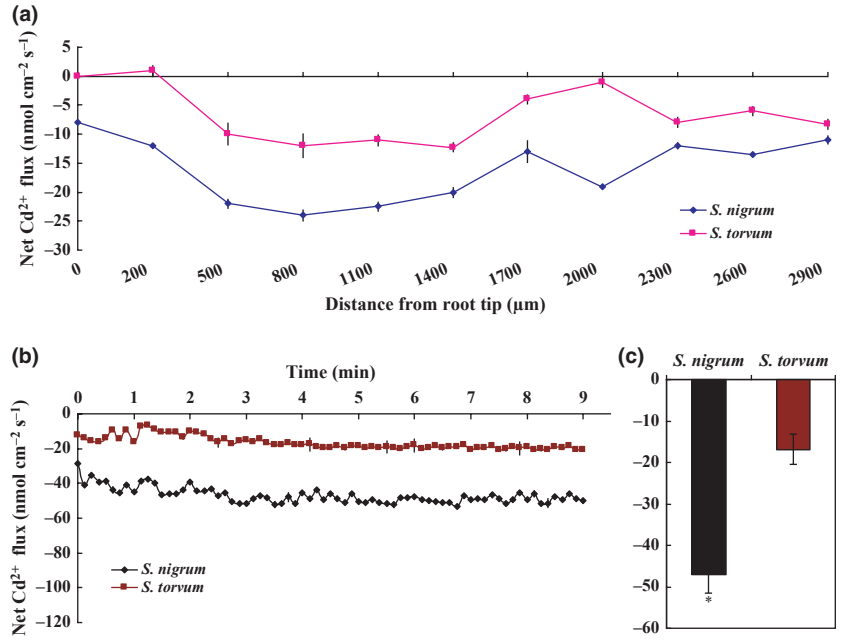

Fig. 2 The net Cd^{2+} fluxes in the roots of *Solanum nigrum* and *Solanum torvum*. (a) Effects of Cd treatment on the net Cd^{2+} fluxes in *S. nigrum* and *S. torvum* roots. (b) Net Cd^{2+} fluxes in *S. nigrum* and *S. torvum* roots. (c) The mean fluxes of Cd^{2+} within the measuring periods. The asterisks indicate the values that were significantly different from those of *S. torvum* ($P < 0.05$). Each point represents the mean of five to six individual roots, and the bars represent the standard error of the mean.

the apex in both of the root tips (Fig. 2a). We also measured the site that was located 500 μm from the root apex, in which a vigorous Cd^{2+} flux was often observed. As shown in Fig. 2(b,c), there were marked differences in the Cd^{2+} fluxes between the two species. The *S. nigrum* roots exhibited a 2.78-fold higher Cd^{2+} influx than that of *S. torvum*, which indicated that a greater Cd uptake capacity existed in the *S. nigrum* roots than in the *S. torvum* roots.

Effects of Cd on micronutrient accumulation

Cadmium toxicity interferes with the accumulation of micronutrients in plants. Because of this, the concentrations of Zn, Fe, and Cu in *S. nigrum* and *S. torvum* were compared (Fig. 3). There were no significant differences in the Cu concentrations between the two species with or without Cd treatment. When the plants were grown without Cd, there were no significant differences in the

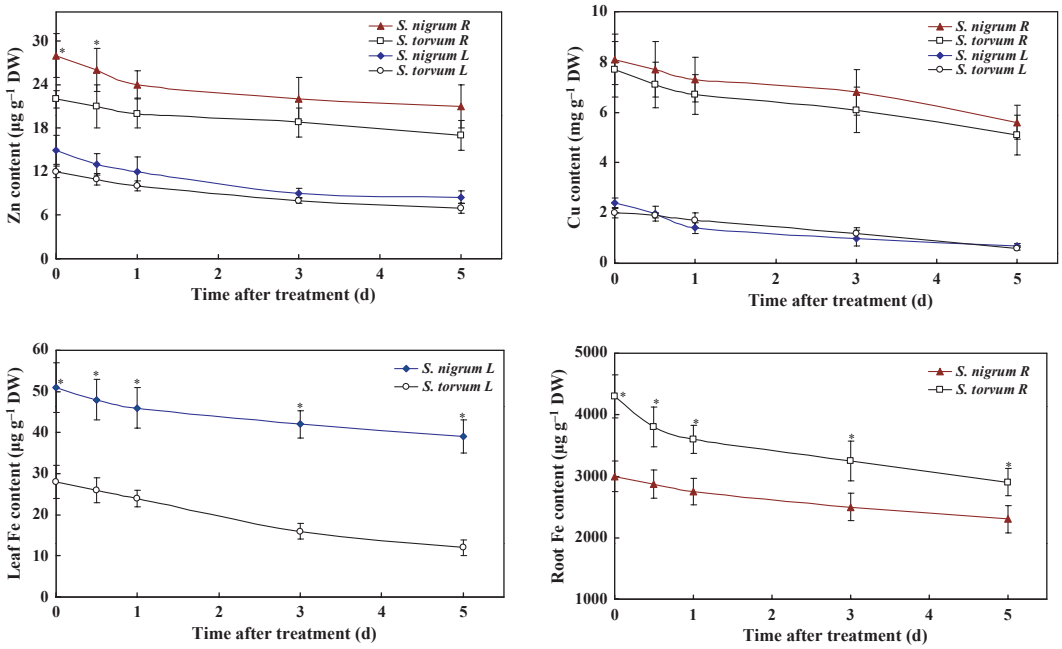

Fig. 3 Metal contents in the cadmium (Cd)-treated *Solanum nigrum* and *Solanum torvum* plants. Symbols: purple triangles, *S. nigrum* roots; white squares, *S. torvum* roots; blue diamonds, *S. nigrum* leaves; white circles, *S. torvum* leaves. The asterisks indicate the values that were significantly different from those of *S. torvum* ($P < 0.05$). Error bars indicate ± SD.

leaf Zn concentrations between the two species, and the accumulation of Zn in the root of *S. nigrum* was higher than in the *S. torvum* roots, whereas the accumulation of Fe was lower in the roots and higher in the leaves of *S. nigrum* compared with *S. torvum*.

Both species showed reduced accumulations of Zn, Fe, and Cu under Cd stress. After 5 d exposure to 50 μM $CdCl_2$, there were no significant differences in the Zn concentrations between the two plant species. However, the Fe concentrations in the *S. nigrum* roots were 1.54-fold lower than those in the *S. torvum* roots, whereas the Fe concentrations in the *S. nigrum* leaves were 2.92-fold higher than those in the *S. torvum* leaves.

Grafts confirmed the efficient root-to-shoot Cd transport in *S. nigrum* roots

It has recently been demonstrated that the low loading rate of Cd into the xylem sap is responsible for the low Cd accumulation in *S. torvum* shoots (Mori *et al.*, 2009). We therefore assumed that the higher Cd accumulation that was observed in the *S. nigrum* leaves was not only the result of the greater Cd uptake capacity of the *S. nigrum* roots, but also possibly the result of a more efficient loading capacity of Cd into the root xylem. Furthermore, we wondered whether Cd loading in the roots was dependent on the shoot genotype. To test these hypotheses, a grafting experiment and subsequently determination of the scions' Cd content were performed in *S. nigrum* and *S. torvum* to analyze the long-distance transport of Cd in whole plants (Fig. 4). After 24 h of treatment, the nongrafted and self-grafted plants showed a virtually identical Cd accumulation. Compared with the self-grafted plants (*S. torvum*/*S. torvum* plants), the *S. torvum* scions from the *S. torvum*/*S. nigrum* plants accumulated a 2.89-fold higher

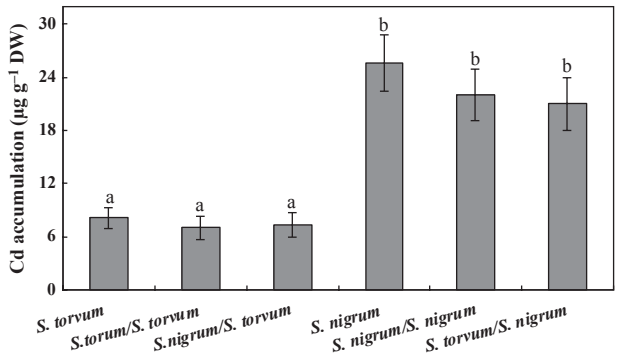

Fig. 4 The effect of grafting on the scions' cadmium (Cd) accumulation in *Solanum nigrum* and *Solanum torvum*. The left side of the division sign (/) represents the scions, and the right side represents the rootstocks. The columns that are labeled with different letters were significantly different at $P < 0.05$. Error bars indicate ± SD.

concentration of Cd, whereas the *S. nigrum* scions from the *S. nigrum*/*S. torvum* plants accumulated only 33.4% of the Cd concentration. It was clear that the Cd content of the scions largely depended on the rootstocks, which suggests that both the Cd uptake capacity in roots and the differential Cd loading capacity into the root xylem are responsible for the differential Cd accumulation between *S. nigrum* and *S. torvum*.

Gene expression analysis

The results in the previous sections indicate that both the Cd uptake capacity and its loading into the root xylem are primarily responsible for Cd accumulation. To further elucidate the mechanisms underlying the differential Cd accumulation in *S. nigrum*

and *S. torvum*, we investigated the transcriptional regulation profiles in the two *Solanum* species roots using a tag-based DGE system. DGE analysis is an extremely sensitive method for the detection of differences in gene expression and facilitates the utilization of nonmodel species. We used a 24 h time course of Cd exposure to evaluate the Cd-responsive genes, because this time course accounted for 50% of the maximum Cd accumulation in the above-ground portions of both species, and the exponential increase stage implied an intense metabolism modulation in plants; and thereby induced a large amount of Cd-responsive gene expression. Twelve DGE libraries were created from three independent biological samples of four treatments and sequenced using Solexa (Illumina) Technology (San Diego, California, USA). After the 3′ adaptor fragments, a few low-quality sequences and several types of impurities were filtered. The sequencing quality evaluation is presented in Fig. S1. The saturation analysis showed that when the sequencing amount reached 2 M or higher, the number of detected genes almost ceased to increase (data not shown). The expressed tags that were obtained from the control and Cd-treated *S. nigrum* and *S. torvum* roots and that aligned to the reference genes generated expression data for 9387, 9211, 10 159, and 10 084 genes, respectively. The genes in all four groups of differential expression are listed in Table S2.

Genes involved in heavy metal transport and detoxification The transcriptional regulation of metal transport and detoxification-related genes that might be involved in the Cd uptake, transport and sequestration processes during Cd treatment were examined (Tables 1, 2). Two metal transporters, an Mg transporter *MGT* and an *HMA* gene, showed constitutively and inducibly higher expression levels in *S. nigrum* roots. A PDR-type ABC transporter *PDR2* showed constitutively higher expression levels in *S. torvum* roots, whereas, it was more highly expressed in *S. nigrum* roots with Cd treatment. Members of the *ZIP* family are involved in the transport of Zn/Fe (Kobae *et al.*, 2004). A ZIP transporter, *IRT1*, was more highly expressed in Cd-treated roots of *S. nigrum*; whereas *IRT2* and a Zn transporter, *ZIP11*, were more highly expressed in the roots of *S. torvum*. The other differentially expressed metal ion transport gene that displayed higher expression levels in *S. torvum* was a Cu transport protein, *COPT5*.

Antioxidant-related genes Cadmium stress induced a marked accumulation of ROS and affected the antioxidant content in the plants (Xu *et al.*, 2009). Fifteen antioxidative stress-related genes were differentially regulated between *S. nigrum* and *S. torvum* during treatment with Cd. Among these genes, six members of the peroxidase superfamily were up-regulated in the *S. torvum* roots when compared with *S. nigrum* under either constitutive (−Cd) or induced (+Cd) conditions. By contrast, five peroxidase family genes, an ascorbate peroxidase gene (*APX1*), an NADPH oxidase gene (*gp91-phox*), a peptidyl-cysteine S-nitrosylation-related gene (*peroxiredoxin-2E*), and a nonsymbiotic hemoglobin gene (ns-*Hb1*) showed higher expression levels in *S. nigrum* roots than in *S. torvum*.

When gene expression levels were compared between the *S. nigrum* and *S. torvum* roots, an antioxidative gene, ns-*Hb1*, was more up-regulated in *S. nigrum* than all of the other genes that were tested (17.4-fold higher expression in *S. nigrum*). The ns-Hb1 protein has a superior affinity for oxygen and its overexpression in plants was shown to increase the ROS scavenging capacity, thereby improving stress tolerance (Borisjuk *et al.*, 2007; Thiel *et al.*, 2011).

Genes involved in metabolic processes The expression levels of eight genes that are involved in amino acid biosynthesis and metabolism were higher in the *S. nigrum* roots than in the *S. torvum* roots with or without Cd treatment. These genes are involved in the biosynthesis and metabolism of several amino acids, such as aromatic amino acids, aspartate, serine, and threonine. Three amino acid transporters also showed higher expression levels in *S. nigrum* roots with or without Cd treatment.

Cadmium toxicity markedly affected carbohydrate metabolism in these plants. Two citrate synthase *CSY* and *CLA* genes, and two malate dehydrogenase *MDH* genes were more highly expressed in the *S. nigrum* roots than in the *S. torvum* roots. Cd treatment also markedly modulated cell wall metabolism processes. Three genes (*RGP9*, *XTH9*, and *EXPA*) that are involved in cell wall metabolism and biosynthesis were more highly expressed in the *S. torvum* roots with or without Cd treatment.

Verification of the DGE results

To verify the gene expression patterns that were observed in the DGE studies by using an independent experimental approach, semiquantitative reverse transcription (RT)-PCR and RT-qPCR analyses were performed for selected genes. We selected *UBQ14*, *18S RNA*, *ACT*, *TUBST1*, *S23*, *RPL8*, and *UBI2* as the candidate reference genes for RT-qPCR normalization. The geNorm software analysis indicates that the expression of *18S RNA* was the most stable in the two *Solanum* species, and the pairwise variation *V* value of *18S RNA*, *ACT*, *UBQ14* and *UBI2* was 0.15 (Fig. S2), which suggested that these genes were suitable reference genes for RT-qPCR normalization. The gene expression levels were normalized using the geometric mean of the four most stable expressed reference gene quantities, as described in the geNorm manual (http://medgen.ugent.be/~jvdesomp/genorm/geNorm_manual.pdf). The results presented in Fig. 5 showed good agreement with the DGE data. The expression levels of *MGT*, *IRT1*, *PDR2*, *HMA*, *ns-Hb1*, *MEE*, and *CYS* genes were higher in *S. nigrum*, whereas *IRT2*, *ZIP11*, and *COPT5* were more highly expressed in *S. torvum* under Cd stress conditions. The high confirmation rate indicates the reliability of our data.

Effect of Fe on leaf Cd tolerance

Cadmium toxicity strongly impaired the seedling growth and led to Fe deficiency. ICP-MS analysis indicated that the accumulation of Fe in *S. torvum* leaves is lower than in *S. nigrum*. To determine whether the lower Fe accumulation is related to the low Cd tolerance in *S. torvum* leaves, we analyzed the impact of

Table 1 Constitutive differences (−Cd; *Solanum nigrum*/*Solanum torvum*) of 4-wk-old plants that were grown in Hoagland solution for 1 d

Unigene	TPM-Snck	TPM-Stck	Stck/Snck	*P*-value	FDR	Annotation	Most related *Arabidopsis* gene
Metal transport and detoxicity							
gnlUGlLes#S50868330	0.51 ± 0.11	191.93 ± 25.46	8.56	7.44E−05	0.000120447	Iron-regulated transporter 2 (IRT2)	IRT2 (AT4G19680.1)
YFR02I11A	2.96 ± 0.11	11.88 ± 1.44	1.99	7.95E−09	1.78E−08	Zinc transporter ZIP11	ZIP11 (AT1G55910.1)
MLF03E07A	1.66 ± 0.68	8.62 ± 3.07	9.82	0	0	Copper transporter 5 (COPT5)	COPT5 (AT5G20650.1)
TVR05N17C	58.50 ± 6.75	180.73 ± 34.94	2.75	0	0	PDR-type ABC transporter 2 (PDR2)	PDR12 (AT1G15520.1)
gnlUGlLes#S50865824	19.44 ± 6.52	0.76 ± 0.03	−4.6	2.55E−30	1.05E−29	Magnesium transporter (MGT)	MGT2 (AT1G16010.1)
PLA08N18C	21.52 ± 0.76	2.13 ± 0.52	−3.35	2.26E−28	9.13E−28	CPx-type heavy metal ATPases (Cu-HMA)	HMA mRNA (AT5G24580.1)
Antioxidant-related genes							
gnlUGlLes#S19872985	1.12 ± 0.45	9.62 ± 3.09	9.99	0	0	Pericarp peroxidase 3	PCA (AT3G49110.1)
TVL29A05A	50.51 ± 20.53	853.98 ± 234.31	4.11	2.60E−13	7.63E−13	Secretory peroxidase	PRXR1 (AT4G21960.1)
gnlUGlLes#S50868621	0.25 ± 0.11	21.14 ± 2.84	11.06	0	0	Cell wall peroxidase	POD mRNA (AT1G05240.1)
SmFL26N14A	19.89 ± 8.16	75.21 ± 9.60	1.85	1.58E−13	4.69E−13	Anionic peroxidase swpa7	POD mRNA (AT4G33420.1)
TVR09D09C	7.70 ± 2.98	88.70 ± 10.77	3.44	4.33E−14	1.36E−13	Peroxidase 16 precursor	POD 16 (AT2G18980.1)
TVR20O05A	24.31 ± 9.77	490.21 ± 68.92	4.24	1.10E−13	3.33E−13	Peroxidase	POD mRNA (AT4G26010.1)
TVR02B24C	0.57 ± 0.33	2337.14 ± 344.27	17.86	0	0	Peroxidase	RCI3 (AT1G05260.1)
OVS01L14C	22.27 ± 1.33	5.81 ± 0.36	−1.91	6.03E−16	2.05E−15	L-ascorbate peroxidase 1 (APX1)	APX3 (AT4G35000)
gnlUGlLes#S5295560	38.32 ± 14.25	2.41 ± 1.72	−11.84	1.43E−72	7.06E−72	gp91-phox	RBOH F (AT1G64060)
gnlUGlLes#S50870409	47.97 ± 4.76	5.39 ± 0.82	−3.13	5.29E−57	2.52E−56	Peroxiredoxin-2E	Peroxiredoxin-2E (AT3G52960)
gnlUGlLes#S50869570	44.09 ± 13.34	3.90 ± 1.42	−3.4	4.77E−55	2.26E−54	Cationic peroxidase 1	POD 52 (AT5G05340)
gnlUGlLes#S19873013	666.81 ± 204.36	21.27 ± 4.42	−4.89	0	0	Peroxidase 27 (POD27)	POD 27 (AT3G01190)
gnlUGlLes#S50868321	16.48 ± 3.53	1.73 ± 0.70	−3.2	2.83E−21	1.05E−20	Peroxidase isoform 1	PRXR1 (AT4G21960)
gnlUGlLes#S50872668	38.78 ± 8.72	10.24 ± 2.63	−1.84	6.57E−25	2.56E−24	Peroxidase 31-like	POD 63 (AT5G40150)
gnlUGlLes#S50870002	1877.96 ± 229.81	0.90 ± 0.16	−10.98	0	0	Nonsymbiotic hemoglobin class 1	HB1 (At2g16060)
Amino acid biosynthesis and metabolism processes							
gnlUGlLes#S50866782	8.90 ± 0.81	2.72 ± 1.45	−9.82	2.19E−18	7.79E−18	Carbamoyl phosphate synthase (CARA)	CARA (AT3G27740)
gnlUGlLes#S50875591	42.71 ± 14.31	3.90 ± 0.92	−3.36	3.51E−52	1.64E−51	Dehydroquinate dehydratase (MEE)	MEE32 (AT3G06350)
gnlUGlLes#S50875554	57.65 ± 2.63	0.36 ± 0.03	−7.33	1.62E−110	8.42E−110	Cysteine desulfurase	NFS1 (AT5G65720)
SmFL26A01A	7.76 ± 1.50	0.77 ± 0.19	−3.32	1.40E−10	3.46E−10	Dihydroxy-acid dehydratase (DHAD)	DHAD (AT3G23940)
gnlUGlLes#S50868067	18.15 ± 3.09	1.55 ± 0.41	−3.54	1.92E−25	7.51E−25	Aspartate aminotransferase-like	ASP5 (AT4G31990)
gnlUGlLes#S50876362	11.35 ± 1.60	0.33 ± 0.16	−10.13	1.41E−22	5.32E−22	SAT1	SERAT2;1 (AT1G55920)
MLF01C11A	62.14 ± 9.31	3.52 ± 1.51	−4	3.71E−88	1.88E−87	DAHP synthase 1 (DHS1)	DHS1 (AT4G39980)
gnlUGlLes#S35431021	58.24 ± 17.54	7.64 ± 2.98	−2.9	1.25E−66	6.11E−66	Chloroplast threonine deaminase 1 (OMR1)	OMR1 (AT3G10050)
SmFL04D23A	15.63 ± 4.79	2.60 ± 0.52	−2.61	5.44E−17	1.90E−16	Serine racemase	SR (AT4G11640)
Amino acid transporter							
SmFL25G05A	25.36 ± 11.52	2.47 ± 0.48	−3.25	4.81E−30	1.98E−29	Amino acid transporter	CAT6 (AT5G04770)
gnlUGlLes#S50875643	11.85 ± 4.03	2.67 ± 0.32	−2.16	7.67E−11	1.93E−10	Amino acid permease 2	AAP2 (AT5G09220)
SmFL12E21A	47.92 ± 9.54	3.38 ± 0.61	−3.83	8.35E−70	4.10E−69	Amino acid transporter	AAP (AT5G41800)
Carbohydrate and Cell wall metabolism processes							
PLA07L14C	21.13 ± 4.79	1.60 ± 0.24	−3.69	3.48E−29	1.42E−28	ATP-citrate synthase (CSY)	CSY4 (AT2G44350.1)
gnlUGlLes#S19872200	125.64 ± 11.09	4.44 ± 1.82	−4.74	2.06E−203	1.13E−202	ATP citrate synthase activity (CLA)	ACLA-3 (AT1G09430.1)
SmFL11P19A	27.18 ± 8.84	2.92 ± 0.46	−3.26	7.32E−36	3.15E−35	Malate dehydrogenase (PMDH)	PMDH1 (AT2G22780)
SmFL29H15A	51.70 ± 12.01	211.68 ± 11.09	2.02	4.45E−13	1.27E−12	RGP2	RGP2 (AT5G15650.1)
TVR04L12C	15.39 ± 1.56	251.57 ± 23.35	4.04	0	0	XTH9	XTH9 (AT4G03210.2)
TVR31P16A	27.67 ± 10.50	249.83 ± 40.49	3.24	3.21E−13	9.31E−13	O-methyltransferase (OMT)	OMT1 (AT5G54160)
TVR34M06C	1.87 ± 1.06	14.48 ± 4.27	10.56	0	0	Expansin (EXPA)	EXLB1 (AT4G17030)

Snck, control for *S. nigrum* roots; Stck, control for *S. torvum* roots; TPM, normalized expression level of genes, mean ± SE, $n = 3$; Stck/Snck, log2 (multiples of differentially expressed); *P*-value, *P*-value from difference test; FDR, false discovery rate.
Orange, up-regulated genes; green, down-regulated genes.

New Phytologist (2012)
www.newphytologist.com

Table 2 Induced differences (+ Cd; *Solanum nigrum*/*S. torvum*) of 4-wk-old plants that were grown in Hoagland solution and treated with 50 μM $CdCl_2$ for 1 d

Unigene	TPM-SntrR	TPM-SttrR	Sttr/Sntr	*P*-value	FDR	Annotation	Most related *Arabidopsis* gene
Metal transport and detoxicity							
gnlUGlLes#S50868330	1.04 ± 0.62	11.25 ± 1.83	10.17	0	0	Iron-regulated transporter 2 (IRT2)	IRT2 (AT4G19680.1)
YFR02I11A	4.16 ± 0.95	123.19 ± 5.33	4.8	3.42E–12	8.33E–12	Zinc transporter ZIP11	ZIP11 (AT1G55910.1)
MLF03E07A	11.38 ± 5.31	39.60 ± 15.91	1.78	0	0	Copper transporter 5 (COPT5)	COPT5 (AT5G20650.1)
gnlUGlLes#S50865824	14.14 ± 0.94	2.31 ± 0.85	–2.54	3.31E–16	1.02E–15	Magnesium transporter (MGT)	MGT2 (AT1G16010.1)
gnlUGlLes#S5295427	56.70 ± 6.36	4.69 ± 1.64	–3.52	1.06E–81	5.08E–81	Iron-regulated transporter 1 (IRT1)	IRT1 (AT4G19690.1)
TVR05N17C	390.34 ± 33.17	180.90 ± 55.27	–1.6	1.49E–12	3.71E–12	PDR-type ABC transporter 2 (PDR2)	PDR12 (AT1G15520.1)
PLA08N18C	13.90 ± 1.95	1.07 ± 0.46	–3.63	3.19E–21	1.08E–20	CPx-type heavy metal ATPases (Cu-HMA)	HMA mRNA (AT5G24580.1)
Antioxidant-related genes							
gnlUGlLes#S19872985	4.43 ± 1.91	58.12 ± 21.08	3.69	6.88E–13	1.75E–12	Pericarp peroxidase 3	PCA (AT3G49110.1)
TVL29A05A	58.13 ± 32.64	624.28 ± 204.68	3.38	6.72E–13	1.72E–12	Secretory peroxidase	PRXR1 (AT4G21960.1)
gnlUGlLes#S50868621	4.21 ± 1.45	38.43 ± 6.99	3.16	3.42E–12	8.34E–12	Cell wall peroxidase	POD mRNA (AT1G05240.1)
TVR09D09C	6.62 ± 3.16	96.94 ± 9.89	13.22	0	0	Peroxidase 16 precursor	POD 16 (AT2G18980.1)
TVR20O05A	8.46 ± 3.46	76.27 ± 4.20	12.9	0	0	Peroxidase	POD mRNA (AT4G26010.1)
TVR02B24C	0.40 ± 0.12	1841.69 ± 267.36	12.35	0.000120589	0.000178528	Peroxidase	RCI3 (AT1G05260.1)
gnlUGlLes#S50874056	64.82 ± 26.52	8.39 ± 3.23	–2.97	1.05E–85	5.05E–85	Peroxidase	POD 59 (AT5G19890)
gnlUGlLes#S50868816	20.19 ± 5.19	6.68 ± 1.13	–1.67	4.40E–14	1.25E–13	Peroxidase 21	POD mRNA (AT2G37130)
OVS01L14C	17.60 ± 4.60	2.96 ± 0.10	–2.5	3.26E–18	1.05E–17	L-ascorbate peroxidase 1 (APX1)	APX3 (AT4G35000)
gnlUGlLes#S5295560	61.25 ± 9.86	5.53 ± 2.04	–3.35	4.15E–81	1.97E–80	gp91-phox	RBOH F (AT1G64060)
gnlUGlLes#S50870409	44.37 ± 3.56	3.84 ± 1.07	–3.44	1.10E–61	4.95E–61	Peroxiredoxin-2E	Peroxiredoxin-2E (AT3G52960)
gnlUGlLes#S50869570	171.31 ± 14.45	4.92 ± 1.40	–5.05	0	0	Cationic peroxidase 1	POD 52 (AT5G05340)
gnlUGlLes#S19873013	1129.83 ± 221.74	0.68 ± 0.20	–10.56	0	0	Peroxidase 27 (POD27)	POD 27 (AT3G01190)
gnlUGlLes#S50868321	14.70 ± 2.62	0.75 ± 0.33	–10.58	1.47E–33	5.71E–33	Peroxidase isoform 1	prxr1 (AT4G21960)
gnlUGlLes#S50870002	1810.39 ± 279.17	0.60 ± 0.24	–17.44	0	0	Nonsymbiotic hemoglobin class 1	HB1 (At2g16060)
Amino acid biosynthesis and metabolism processes							
gnlUGlLes#S50875591	62.47 ± 10.46	8.83 ± 3.65	–12.61	4.03E–134	2.07E–133	Dehydroquinate dehydratase (MEE)	MEE32 (AT3G06350)
gnlUGlLes#S50875554	53.72 ± 3.99	0.65 ± 0.15	–6.33	2.59E–108	1.29E–107	Cysteine desulfurase	NFS1 (AT5G65720)
SmFL26A01A	12.89 ± 3.14	0.87 ± 0.15	–3.94	1.44E–21	4.89E–21	Dihydroxy-acid dehydratase (DHAD)	DHAD (AT3G23940)
gnlUGlLes#S50868067	20.30 ± 7.42	1.91 ± 0.64	–3.43	8.41E–31	3.19E–30	Aspartate aminotransferase-like	ASP5 (AT4G31990)
gnlUGlLes#S50876362	52.83 ± 7.54	5.79 ± 2.32	–3.05	5.03E–65	2.29E–64	SAT1	SERAT2;1 (AT1G55920)
MLF01C11A	31.22 ± 1.70	3.54 ± 1.17	–3.03	3.76E–39	1.52E–38	DAHP synthase 1 (DHS1)	DHS1 (AT4G39980)
gnlUGlLes#S35431021	60.23 ± 23.73	9.98 ± 4.07	–2.59	3.60E–68	1.66E–67	Chloroplast threonine deaminase 1 (OMR1)	OMR1 (AT3G10050)
SmFL04D23A	18.57 ± 4.78	4.27 ± 0.17	–2.19	4.30E–18	1.38E–17	Serine racemase	SR (AT4G11640)
Amino acid transporter							
SmFL25G05A	18.81 ± 5.80	1.25 ± 0.17	–3.75	7.60E–27	2.75E–26	Amino acid transporter	CAT6 (AT5G04770)
gnlUGlLes#S50875643	9.91 ± 3.70	0.78 ± 0.21	–3.72	2.00E–17	6.34E–17	Amino acid permease 2	AAP2 (AT5G09220)
SmFL12E21A	28.21 ± 3.23	4.03 ± 1.10	–2.76	1.21E–33	4.70E–33	Amino acid transporter	AAP (AT5G41800)
Carbohydrate and cell wall metabolism processes							
PLA07L14C	73.60 ± 12.57	4.25 ± 1.60	–4.18	1.39E–116	7.01E–116	ATP-citrate synthase (CSY)	CSY4 (AT2G44350.1)
gnlUGlLes#S19872200	434.54 ± 69.53	43.53 ± 17.01	–3.25	0	0	ATP citrate synthase activity (CLA)	ACLA-3 (AT1G09430.1)
TVR36E09W	4.62 ± 1.27	1.19 ± 0.22	–1.97	5.01E–05	7.65E–05	Malate dehydrogenase (MDH)	MDH (AT5G58330)
gnlUGlLes#S51712555	307.67 ± 15.05	104.26 ± 12.76	–1.58	4.09E–167	2.15E–166	Malate dehydrogenase (mMDH)	mMDH1 (AT1G53240)
SmFL29H15A	45.34 ± 17.77	147.96 ± 27.76	1.65	4.60E–13	1.19E–12	RGP2	RGP2 (AT5G15650.1)
TVR04L12C	9.57 ± 1.41	67.15 ± 6.27	2.76	0	0	XTH9	XTH9 (AT4G03210.2)
TVR34M06C	43.72 ± 24.37	659.61 ± 237.82	3.9	8.44E–14	2.34E–13	Expansin (EXPA)	EXLB1 (AT4G17030)

Sntr, Cd-treated *S. nigrum* roots; Sttr, Cd-treated *S. torvum* roots; TPM, normalized expression level of genes, mean ± SE, $n = 3$; Sttr/Sntr, log2 (multiples of differentially expressed); *P*-value, *P*-value from difference test; FDR, false discovery rate.
Orange, up-regulated genes; green, down-regulated genes.

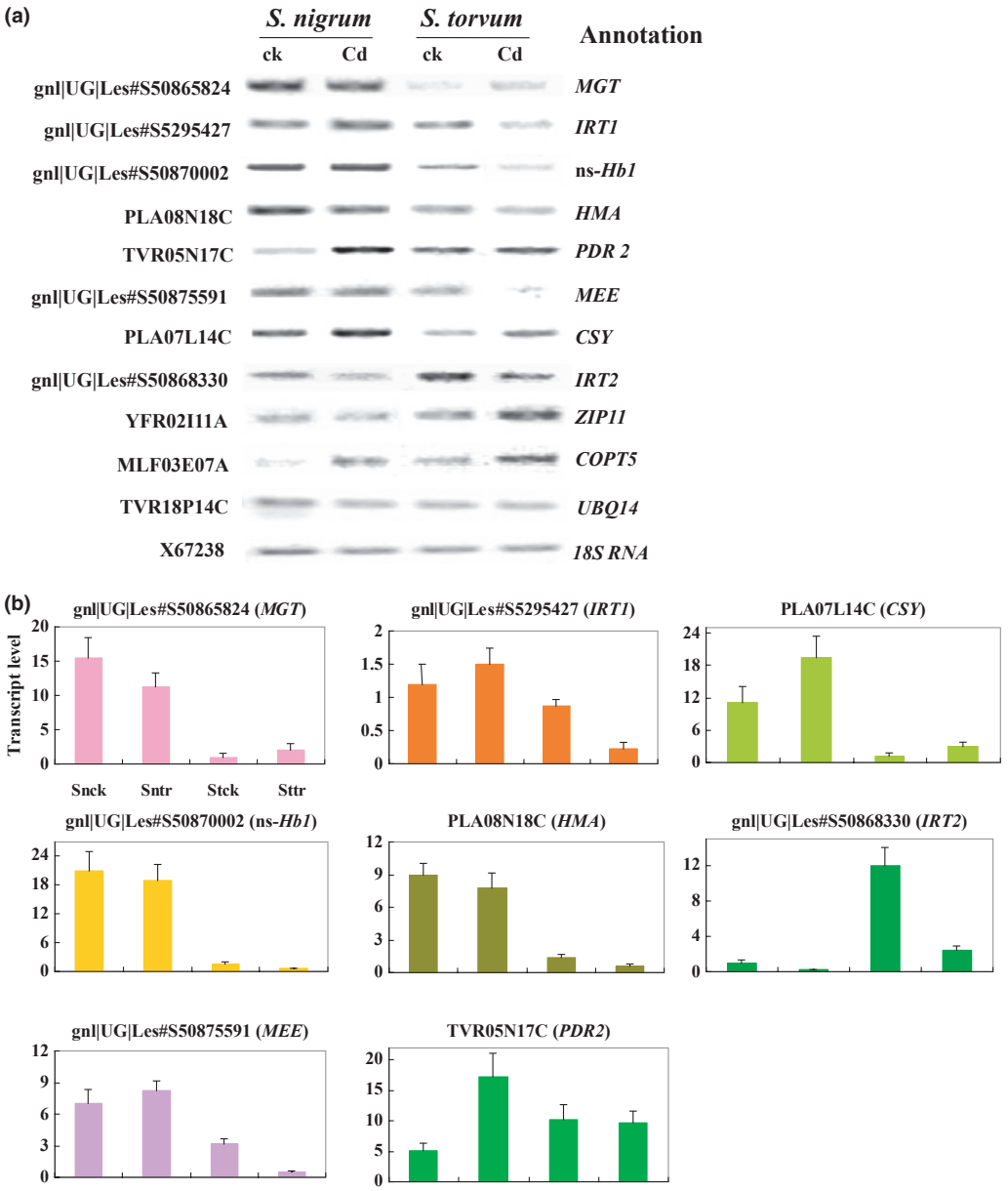

Fig. 5 Semiquantitative reverse transcription polymerase chain reaction (RT-PCR) (a) and quantitative RT-PCR (b) confirmation of the digital gene expression (DGE) data from *Solanum nigrum* and *Solanum torvum*. ck, 4-wk-old untreated control; Cd, treated with 50 μM $CdCl_2$ for 24 h. Bars represent the 95% CI of the normalized expression.

Fe supply on leaf physiology in Cd-treated plants. Supplementation with Fe did not affect Cd accumulation in the leaves of the two species after 5 d of treatment. Fe deficiency increased Cd accumulation in *S. nigrum* leaves after 5 d of treatment; however, it did not affect Cd accumulation in *S. torvum* leaves (Fig. 6). The *Pn* of both species continued to decrease during the exposure to 50 μM Cd stress. Fe supplementation did not affect the *Pn* in the Cd-treated *S. nigrum* plant; however, the rate of reduction was lower in Fe-supplemented *S. torvum* plants (Fig. 7a). By contrast, Fe deficiency reduced the *Pn* to a greater extent in both *S. nigrum* and *S. torvum* than did Cd treatment alone. Similarly, the O_2^- and H_2O_2 accumulation in leaves of *S. torvum* supplemented with 50 μM Fe was lower than with Cd treatment alone, and Fe deficiency induced higher O_2^- and H_2O_2 accumulation in both *S. nigrum* and *S. torvum* leaves (Fig. 7b,c). Consistent with the phenomenon of ROS accumulation, Fe deficiency increased the MDA concentration and electrolyte leakage, whereas Fe supplementation effectively reduced the MDA concentration and electrolyte leakage in leaves of Cd-treated *S. torvum* (Fig. 8a,b), indicating that there is a positive effect of Fe supplementation on alleviating Cd-induced oxidative damage in *S. torvum* plants.

These results indicate that Fe deficiency increased Cd accumulation only in *S. nigrum* leaves after 5 d of treatment. *IRT1* and *IRT2* are two important Fe transporter genes involved in the Cd accumulation and tolerance in plants (Vert *et al.*, 2002, 2009). To explore the possible involvement of these genes in modulating

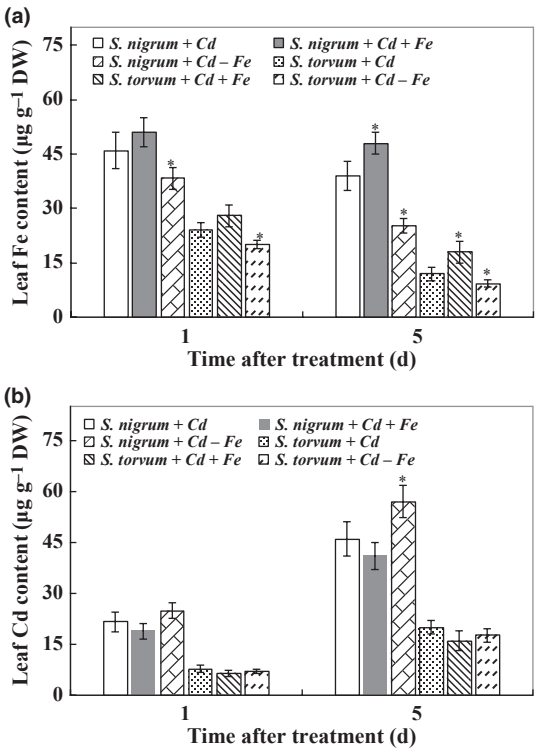

Fig. 6 Effects of Fe supplementation and deficiency on Cd accumulation in *Solanum nigrum* and *Solanum torvum* leaves. The leaf Fe accumulation (a) and the leaf Cd accumulation (b) were recorded separately at 1 and 5 d after Cd treatment. Asterisks indicate values significantly different from those of the plants treated with Cd alone ($P < 0.05$). Error bars indicate ± SD.

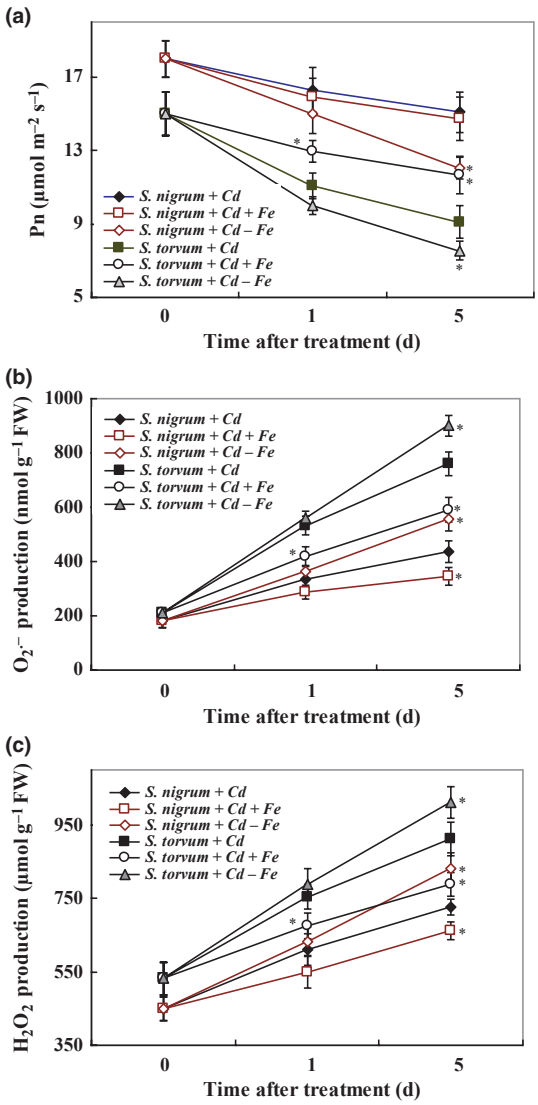

Fig. 7 Effects of Fe supplementation and deficiency on Cd tolerance in *Solanum nigrum* and *Solanum torvum* leaves. Photosynthetic rate (*Pn*) (a), production of superoxide (O_2^-) (b) and hydrogen peroxide (H_2O_2) (c) were recorded separately at 0, 1, and 5 d after Cd treatment. Asterisks indicate values significantly different from those of the plants treated with Cd alone ($P < 0.05$). Error bars indicate ± SD.

the differential Fe/Cd accumulation in the two species, we examined the gene expression of *IRT1* and *IRT2* in the roots of plants treated with Cd or without Fe supply. As shown in Fig. 9, both Cd treatment and Fe deficiency up-regulated the expression of *IRT1* in *S. nigrum*. By contrast, Cd treatment and Fe deficiency down-regulated the expression of *IRT1* and *IRT2* in the roots of *S. torvum*. The results of these experiments are discussed in the following section.

Discussion

The transcriptional regulation of genes plays an important role in metal homeostasis (Wintz *et al.*, 2003). The majority of transcriptomics analyses of differential Cd accumulation are based on the comparative analysis between hyperaccumulator and related nonhyperaccumulator species. The reported Cd hyperaccumulators are also Zn hyperaccumulators, which suggests that Cd and Zn accumulation at least partially rely on common genetic determinants (Xing *et al.*, 2008; Verbruggen *et al.*, 2009). However, in this study, we found that although *S. torvum* accumulated lower Cd, the Zn concentration was unaffected, implying that a specific mechanism exists in *S. torvum* for low Cd accumulation. Therefore, in this study, we chose the Cd accumulator *S. nigrum* and its low Cd-accumulating relative *S. torvum* for comparative transcriptome analysis. Also, to the best of our knowledge, this study represents the first transcriptome analysis of *S. nigrum* using a tag-based DGE system, which allowed us to identify new genes that may contribute to the differential Cd accumulation and tolerance phenotype of the two *Solanum* species.

The enhanced expression of heavy metal transporter genes in hyperaccumulators is universal and is regarded as a central characteristic of heavy metal hyperaccumulation (Weber *et al.*, 2006; Verbruggen *et al.*, 2009). However, in this study, we found that several metal transporters showed higher expression in *S. torvum*, which suggests that these genes are involved in low Cd accumulation. These results are discussed in the following. Our study supports the idea that the modulation of Cd distribution in plants and intracellular redistribution (via sequestrate metal in vacuoles or organelles in roots or long-distance transport from root to

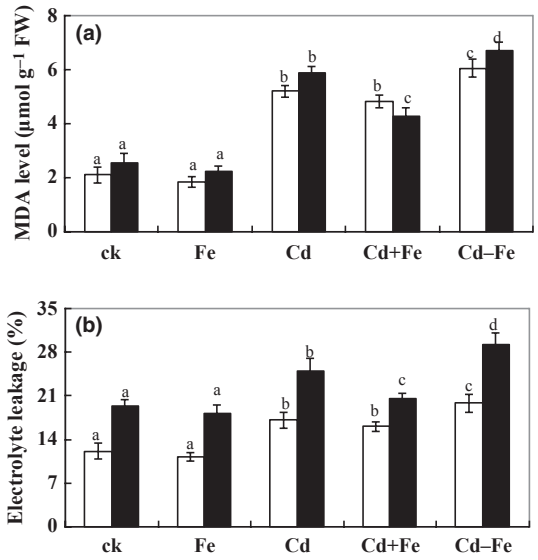

Fig. 8 Effects of Fe supply on Cd tolerance in *Solanum nigrum* (open bars) and *Solanum torvum* (closed bars). Malondialdehyde (MDA) content (a) and electrolyte leakage (b) in the leaves of 4-wk-old *S. nigrum* and *S. torvum* plants that were grown in Hoagland solution treated with 50 μM $CdCl_2$ (Cd), 50 μM Fe (Fe), 50 μM $CdCl_2$ plus 50 μM Fe (Cd+Fe) or Fe deficiency plus 50 μM $CdCl_2$ (Cd–Fe) for 5 d. The different letters indicate the values that were significantly different from their appropriate controls (without Cd) at $P < 0.05$. Error bars indicate ± SD.

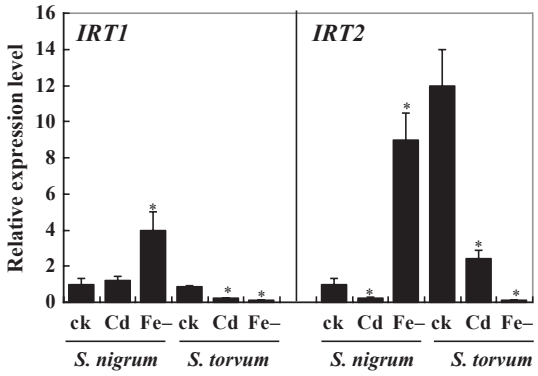

Fig. 9 The expression profile of *IRT1* and *IRT2* were monitored by RT-qPCR in the 4-wk-old *Solanum nigrum* and *Solanum torvum* plants grown under conditions without (ck) and with 50 μM $CdCl_2$ (Cd) as well as without Fe supply (Fe–) at 1 d. The asterisks indicate the values that were significantly different from their appropriate controls (ck) ($P < 0.05$) Error bars indicate ± SD.

shoot and storage in leaf vacuoles) play a vital role in differential Cd accumulation.

The Cd accumulator *S. nigrum* was more tolerant to Cd stress than *S. torvum* (Figs 1a, 7, 8). The leaf Cd accumulation was threefold higher in *S. nigrum* than in *S. torvum*, which demonstrates the high Cd detoxification capability of *S. nigrum*. A previous study indicated that, although *S. torvum* accumulated similar Cd concentrations in its roots, it accumulated lower Cd concentrations in its shoots compared with eggplant (*S. melongena*; Arao *et al.*, 2008), which suggested that the roots contained a vital factor that controlled the Cd loading capacity into the xylem. In support of this result, by using horticultural and physiological approaches, we demonstrated that the root-to-shoot translocation plays a major role in the differential Cd accumulation between *S. nigrum* and *S. torvum*. Subsequently, our transcriptomic studies offered some insight into the molecular mechanisms that potentially mediate these differences in Cd accumulation.

Several studies have indicated that a high antioxidative capacity is responsible for heavy metal hyperaccumulation in plants (Schutzendubel & Polle, 2002; Cho & Seo, 2005; Wang *et al.*, 2008). *S. nigrum* accumulated lower ROS concentrations than *S. torvum* in the presence of Cd (Fig. 7b,c), which suggests that *S. nigrum* has a high free radical scavenging capacity. However, in this study, we found that most differentially expressed antioxidant-related genes are peroxidase family genes. Other several important antioxidative enzyme genes, such as *SOD* and *CAT*, did not show differential expression between the two species. The transcriptome analysis also identified an ns-*Hb1* gene, which may function as an antioxidant. Of all of the genes that were tested, ns-*Hb1* was the most up-regulated gene in the *S. nigrum* roots compared with that in the *S. torvum* roots. Plant ns-Hbs function in a variety of cellular processes and its overexpression in plants were shown to enable the cell to maintain high quantities of ATP when under stress (Borisjuk *et al.*, 2007; Thiel *et al.*, 2011). Previous studies indicated that purified recombinant *Arabidopsis* ns-Hbs displayed intrinsic peroxidase-like activity (Sakamoto *et al.*, 2004). Overexpression of *GhHb1* gene decreased the concentration of cellular NO in *Arabidopsis* seedlings (Qu *et al.*, 2006), indicating that ns-Hbs plays a role in modulating the NO concentrations and the ratio of H_2O_2/NO in the defense process (Igamberdiev *et al.*, 2004; Qu *et al.*, 2006). In this study, we found that *S. nigrum* roots accumulated a higher level of ns-*Hb1* transcript than that in *S. torvum*. Moreover, we found that Cd treatment further reduced ns-*Hb1* expression in *S. torvum* roots but did not have a significant effect on ns-*Hb1* expression in *S. nigrum* roots (Table S1). These findings imply that this *Hb1* gene may play an important role in the Cd stress-response process of *S. nigrum* seedlings. Interestingly, we also found that a peptidyl-cysteine S-nitrosylation-related gene, *peroxiredoxin-2E*, was more highly expressed in *S. nigrum* roots. The post-translational modification (S-nitrosylation) of cysteine thiol to form nitrosothiol (SNO) is a key feature of NO and is coupled to the stimulation of all isoforms of NO synthase (Stamler, 1994; Stamler *et al.*, 2001; Liu *et al.*, 2004). The majority of all NO-affected proteins seem to be regulated by the S-nitrosylation of a single critical Cys residue (Lindermayr *et al.*, 2005). Our previous studies have indicated that NO is associated with long-term Zn and Cd tolerance and accumulation in *S. nigrum* seedlings (Xu *et al.*, 2010, 2011). The enhanced expression of the *peroxiredoxin-2E* gene in *S. nigrum* suggests that the gene may be involved in modulating Cd tolerance and accumulation by the NO signaling pathway and requires further investigation.

Transcriptome analysis also revealed that an Asp biosynthesis-related gene (*ASP*), a cysteine desulfurase gene (*NFS*) that can

catalyze Cys to Ala, an aromatic amino acid biosynthesis-related gene (*MEE*), and other five amino acid metabolism-related genes showed higher expression in *S. nigrum* than in *S. torvum*, implying that the Cd response in amino acid biosynthesis and metabolism is greater in the roots of *S. nigrum* than in the roots of *S. torvum*. Amino acid accumulation is a central plant response to heavy metal exposure. Further metabolomic analysis of amino acids will help to elucidate the roles of amino acids in controlling Cd tolerance and accumulation in hyperaccumulating and low Cd-accumulating plants.

The ZIP family transporters are the important Zn/Fe transporters (Talke *et al.*, 2006; Plaza *et al.*, 2007) and the COPT family transporters are the important Cu transport proteins (Sancenon *et al.*, 2003; Penarrubia *et al.*, 2010). Two ZIP transporters (*IRT2* and *ZIP11*) and a COPT transporter (*COPT5*) displayed a lower level of gene expression in *S. nigrum* than in *S. torvum*. *IRT2* may compartmentalize Fe/Cd into vesicles, to prevent toxicity by excess free Fe/Cd in the cytosol (Vert *et al.*, 2009). The results were consistent with the observed phenotype of high Fe accumulation in *S. torvum* roots and implied that *S. nigrum* may rely on other transporters to acquire Cd. *ZIP11* is an endomembrane system-located Zn/Cd transporter (Plaza *et al.*, 2007; Antosiewicz *et al.*, 2008). *COPT5* is located in the tonoplast and functions as a vacuolar Cu transporter (Klaumann *et al.*, 2011). An *Arabidopsis copt5* mutant showed markedly reduced root growth under Cd toxicity (Klaumann *et al.*, 2011), which implies that *COPT5* is also involved in Cd tolerance in plants. High expression of *IRT2*, *ZIP11*, and *COPT5* in *S. torvum* roots may promote Cd into the vacuolar or endomembrane systems, thereby increasing root Cd sequestration and reducing Cd transport from the roots to the shoots.

In this study, three heavy metal transporters, *PDR2*, *IRT1*, and an *HMA* transporter, showed higher expression in Cd-treated *S. nigrum* roots than in *S. torvum* roots. *IRT1* is the main route of Fe entry into the plant and mediates the accumulation of additional metal ions (Vert *et al.*, 2002). Because *irt1* mutation is lethal, it is clear that no other *ZIP* gene can substitute for its loss. Even overexpression of *IRT2*, which is the closest homolog of *IRT1*, cannot compensate for the loss of *IRT1* (Varotto *et al.*, 2002). *IRT1* may also be involved in the high-affinity Cd uptake in *Thlaspi caerulescens* Ganges roots (Lombi *et al.*, 2002). *PDR2* is a member of the pleiotropic drug resistance (PDR) subfamily of the ATP-binding cassette (ABC) family of transporters. In *Arabidopsis*, two *PDR* genes, *AtPDR8* and *AtPDR12*, have been suggested to transport heavy metal ions and confer Cd and Pb resistance in *Arabidopsis* (Lee *et al.*, 2005; Kim *et al.*, 2007). The most closely related *Arabidopsis* gene to the *Solanum PDR2* is *AtPDR12*, which suggests that the *Solanum PDR2* gene may be involved in heavy metal resistance and transmembrane transport in plants. Members of the *HMA* family are thought to be involved in the transport of heavy metals (Axelsen & Palmgren, 2001), and several *HMA* genes have been shown to be involved in heavy metal long-distance transport and detoxification (Hussain *et al.*, 2004; Wong & Cobbett, 2009). *HMA2* has been suggested to transport Zn and Cd in *Arabidopsis* (Wong *et al.*, 2009). *TcHMA3* plays a key role in the extreme Cd tolerance in *T. caerulescens* (Ueno *et al.*, 2011). *HMA4* is responsible for the efficient xylem loading of Cd (Bernard *et al.*, 2004; Verret *et al.*, 2004) and has been implicated as a key gene in Cd hyperaccumulator species. However, several similar papers failed to phenocopy Cd hyperaccumulation by overexpressing *HMA4* (Hanikenne *et al.*, 2008; Barabasz *et al.*, 2010, 2012; Siemianowski *et al.*, 2011), which suggests that Cd hyperaccumulation and tolerance are the results of many gene networks working simultaneously. In this study, an *HMA* gene showed higher expression in *S. nigrum* roots than in *S. torvum* roots under Cd toxicity, which suggests that the gene is linked to Cd accumulation and tolerance in *S. nigrum*. The most closely related *Arabidopsis* gene of the *Solanum HMA* is a heavy metal transport/detoxification domain-containing protein (AT5G24580). However, the characterization of the *Arabidopsis HMA* gene remains unclear and requires further investigation.

Compared with *S. torvum*, *S. nigrum* roots accumulated only 20% more Cd; however, the leaves accumulated 179% more Cd, which indicates that a low Cd long-distance transport rate is an important mechanism for low Cd accumulation in *S. torvum*. Yamaguchi *et al.* (2011) reported that the barrier function of the root endodermal Casparian band is one mechanism that is responsible for low Cd loading into the stele in *S. torvum*. In this study, several Casparian band biosynthesis-related genes, including *RGP2* (UDP-glucose: protein transglucosylase), *XTH9* (xyloglucan endotransglucosylase-hydrolase), and *OMT1* (O-methyltransferase) that is involved in Casparian band suberin biosynthesis (Held *et al.*, 1993), displayed higher constitutive expression levels in *S. torvum* roots. A metabolite analysis also identified an amino acid that is an important component of the Casparian band, hydroxy-L-proline (Hyp), and shows greater abundance in the Cd-treated *S. torvum* roots (data not shown). Although our present results, which were obtained from the transcriptome and metabolite analyses, supported this hypothesis, we did not observe any morphological differences between the roots' endodermal Casparian bands of the two *Solanum* species (data not shown). In addition, it is difficult to explain why only Cd and Fe transport was restrained, while Zn and Cu transport was unaffected. Our study showed that during Cd treatment, no significant differences in Zn accumulation existed in *S. torvum* and *S. nigrum*. However, *S. torvum* accumulated a higher Fe concentration in the roots and a lower Fe in the leaves. These results suggest that *S. torvum* has a lower capacity of Fe loading into the xylem, which thereby limited its long-distance root-to-shoot transport. A similar phenotype of low Cd and Fe accumulation in *S. torvum* leaves implies that the modulating or transport pathways that were responsible for Cd and Fe loading into the xylem were similar.

Cadmium toxicity led to Fe deficiency in plants. Decreased Fe accumulation in leaves magnified the malfunction of the photosynthetic system and subsequent oxidative damage (Siedlecka *et al.*, 1997; Solti *et al.*, 2008). In this study, we found that the accumulation of Fe in *S. torvum* leaves is lower than that in *S. nigrum*. Therefore, we hypothesize that low Fe accumulation may be related to the high Cd sensitivity in *S. torvum* leaves compared with *S. nigrum*. Further study on the supplementation with Fe in Cd-treated plants supported the assumption.

Supplementation with Fe effectively improved the *Pn* and reduced ROS accumulation in *S. torvum* plants, thereby increasing Cd tolerance in *S. torvum* leaves. However, we found that Fe supplementation did not affect Cd accumulation in leaves after 5 d of treatment; we therefore propose that the Fe-alleviated oxidative damage induced by Cd is a direct effect of Fe supply.

Iron deficiency increased Cd accumulation solely in *S. nigrum* leaves. This result is in agreement with previous reports by Lombi *et al.* (2002), who found that Cd uptake was significantly enhanced by Fe deficiency in the hyperaccumulator *T. caerulescens* Ganges, but not in the nonaccumulator *T. caerulescens* Prayon ecotype. The quantitative RT-PCR analysis of two Fe transporters, *IRT1* and *IRT2*, indicated that the abundance of these mRNAs were higher in *S. nigrum* roots under Fe-deficient conditions than in *S. torvum* roots. Fe deficiency markedly induced the expression of *IRT1* and *IRT2* in *S. nigrum* roots, whereas it depressed the expression of these genes in *S. torvum* roots. *IRT1* is localized in the plasma membrane, and the high expression of *IRT1* increased Cd/Fe uptake in *S. nigrum* roots. However, the elevated expression level of *IRT2* may result in Cd/Fe sequestration in root vacuoles to maintain a relatively low cellular Cd concentration in the shoots of *S. torvum*. Additionally, the different responsive mechanisms of the transporter genes to Fe deficiency may be responsible for the differential uptake and redistribution of metals in the two *Solanum* species. This topic requires extensive further analysis.

In summary, our data indicated that *S. nigrum*, which is a Cd accumulator, has a higher ability to promote root-to-shoot Cd translocation than its relative, the low Cd accumulator *S. torvum*. Differential responsive mechanisms of the transporter genes to Fe deficiency induced by Cd might be responsible for differential uptake and redistribution of Cd/Fe in the two *Solanum* species. On the other hand, Cd accumulation is a complex biological process that is involved in the integrated gene modulation network and coordinated regulation between roots and leaves. In the present study, we only focused on Cd uptake and translocation in roots. The remobilization of Cd through the phloem has been demonstrated to play a role in modulating Cd distribution and accumulation in plants (Reid *et al.*, 2003; Tanaka *et al.*, 2003; Grant *et al.*, 2008). Further studies regarding the molecular mechanisms of Cd exclusion through the phloem would provide further insight into reducing Cd accumulation in plants.

Acknowledgements

The authors would like to thank the Germplasm Bank of Wild Species in Southwest China for providing the *S. nigrum* and *S. torvum* seeds. This work was supported by the China National Natural Sciences Foundation (31170228).

References

Antosiewicz DM, Sirko A, Sowiński P. 2008. Trace element transport in plants. In: Prasad MNV, eds. *Trace elements as contaminants and nutrients: consequences in ecosystems and human health*. Hoboken, NJ, USA: John Wiley & Sons, Inc, 413–448.

Arao T, Takeda H, Nishihara E. 2008. Reduction of cadmium translocation from roots to shoots in eggplant (*Solanum melongena*) by grafting onto *Solanum torvum* rootstock. *Soil Science and Plant Nutrition* **54**: 555–559.

Axelsen KB, Palmgren MG. 2001. Inventory of the superfamily of P-type ion pumps in *Arabidopsis*. *Plant Physiology* **126**: 696–706.

Barabasz A, Krämer U, Hanikenne M, Rudzka J, Antosiewicz DM. 2010. Metal accumulation in tobacco expressing *Arabidopsis halleri* metal hyperaccumulation gene depends on external supply. *Journal of Experimental Botany* **61**: 3057–3067.

Barabasz A, Wilkowska A, Ruszczyńska A, Bulska E, Hanikenne M, Czarny M, Krämer U, Antosiewicz DM. 2012. Metal response of transgenic tomato plants expressing P1B-ATPase. *Physiologia Plantarum* **145**: 315–331.

Ben Amor N, Hamed KB, Debez A, Grignon C, Abdelly C. 2005. Physiological and antioxidant responses of the perennial halophyte *Crithmum maritimum* to salinity. *Plant Science* **168**: 889–899.

Bernard C, Roosens N, Czernic P, Lebrun M, Verbruggen N. 2004. A novel CPx-ATPase from the cadmium hyperaccumulator *Thlaspi caerulescens*. *FEBS letters* **569**: 140–148.

Besson-Bard A, Gravot A, Richaud P, Auroy P, Duc C, Gaymard F, Taconnat L, Renou JP, Pugin A, Wendehenne D. 2009. Nitric oxide contributes to cadmium toxicity in Arabidopsis by promoting cadmium accumulation in roots and by up-regulating genes related to iron uptake. *Plant Physiology* **149**: 1302–1315.

Borisjuk L, Macherel D, Benamar A, Wobus U, Rolletschek H. 2007. Low oxygen sensing and balancing in plant seeds – a role for nitric oxide. *New Phytologist* **176**: 813–823.

Bustin SA, Benes V, Garson JA, Hellemans J, Huggett J, Kubista M, Mueller R, Nolan T, Pfaffl MW, Shipley GL *et al.* 2009. The MIQE guidelines: minimum information for publication of quantitative real-time PCR experiments. *Clinical Chemistry* **55**: 611–622.

Chen A, Komives EA, Schroeder JI. 2006. An improved grafting technique for mature Arabidopsis plants demonstrates long-distance shoot-to-root transport of phytochelatins in Arabidopsis. *Plant Physiology* **141**: 108–120.

Cho UH, Seo NH. 2005. Oxidative stress in *Arabidopsis thaliana* exposed to cadmium is due to hydrogen peroxide accumulation. *Plant Science* **168**: 113–120.

Clemens S, Antosiewicz DM, Ward JM, Schachtman DP, Schroeder JI. 1998. The plant cDNA *LCT1* mediates the uptake of calcium and cadmium in yeast. *Proceedings of the National Academy of Sciences, USA* **95**: 12043–12048.

Cohen CK, Fox TC, Garvin DF, Kochian LV. 1998. The role of iron-deficiency stress responses in stimulating heavy-metal transport in plants. *Plant Physiology* **116**: 1063–1072.

Freeman JL, Tamaoki M, Stushnoff C, Quinn CF, Cappa JJ, Devonshire J, Fakra SC, Marcus MA, McGrath SP, Van Hoewyk D *et al.* 2010. Molecular mechanisms of selenium tolerance and hyperaccumulation in *Stanleya pinnata*. *Plant Physiology* **153**: 1630–1652.

Grant CA, Clarke JM, Duguid S, Chaney RL. 2008. Selection and breeding of plant cultivars to minimize cadmium accumulation. *Science of the Total Environment* **390**: 301–310.

Hanikenne M, Talke IN, Haydon MJ, Lanz C, Nolte A, Motte P, Kroymann J, Weigel D, Krämer U. 2008. Evolution of metal hyperaccumulation required cis-regulatory changes and triplication of *HMA4*. *Nature* **453**: 391–395.

Held BM, Wang H, John I, Wurtele ES, Colbert JT. 1993. An mRNA putatively coding for an O-methyltransferase accumulates preferentially in maize roots and is located predominantly in the region of the endodermis. *Plant Physiology* **102**: 1001–1008.

Hoagland DR, Arnon DI. 1950. The water-culture method for growing plants without soil. *California Agriculture Experiment Station Circular* **347**, Berkeley, CA, USA.

Hussain D, Haydon MJ, Wang Y, Wong E, Sherson SM, Young J, Camakaris J, Harper JF, Cobbett CS. 2004. P-type ATPase heavy metal transporters with roles in essential zinc homeostasis in *Arabidopsis*. *Plant Cell* **16**: 1327–1339.

Igamberdiev AU, Seregelyes C, Manach N, Hill RD. 2004. NADH-dependent metabolism of nitric oxide in alfalfa root cultures expressing barley hemoglobin. *Planta* **219**: 95–102.

Kim DY, Bovet L, Maeshima M, Martinoia E, Lee Y. 2007. The ABC transporter *AtPDR8* is a cadmium extrusion pump conferring heavy metal resistance. *Plant Journal* **50**: 207–218.

Klaumann S, Nickolaus SD, Fürst SH, Starck S, Schneider S, Ekkehard Neuhaus H, Trentmann O. 2011. The tonoplast copper transporter COPT5 acts as an exporter and is required for interorgan allocation of copper in *Arabidopsis thaliana*. *New Phytologist* **192**: 393–404.

Kobae Y, Uemura T, Sato MH, Ohnishi M, Mimura T, Nakagawa T, Maeshima M. 2004. Zinc transporter of *Arabidopsis thaliana AtMTPl* is localized to vacuolar membranes and implicated in zinc homeostasis. *Plant and Cell Physiology* **45**: 1749–1758.

Lee M, Lee K, Lee J, Noh EW, Lee Y. 2005. *AtPDR12* contributes to lead resistance in *Arabidopsis*. *Plant Physiology* **138**: 827–836.

Lindermayr C, Saalbach G, Durner J. 2005. Proteomic identification of S-nitrosylated proteins in *Arabidopsis*. *Plant Physiology* **137**: 921–930.

Liu L, Yan Y, Zeng M, Zhang J, Hanes MA, Ahearn G, McMahon TJ, Dickfeld T, Marshall HE, Que LG *et al.* 2004. Essential roles of S-nitrosothiols in vascular homeostasis and endotoxic shock. *Cell* **116**: 617–628.

Lombi E, Tearall KL, Howarth JR, Zhao FJ, Hawkesford MJ, McGrath SP. 2002. Influence of iron status on cadmium and zinc uptake by different ecotypes of the hyperaccumulator *Thlaspi caerulescens*. *Plant Physiology* **128**: 1359–1367.

Lux A, Martinka M, Vaculik M, White PJ. 2011. Root responses to cadmium in the rhizosphere: a review. *Journal of Experimental Botany* **62**: 21–37.

Ma WW, Xu WZ, Xu H, Chen YS, He ZY, Ma M. 2010. Nitric oxide modulates cadmium influx during cadmium-induced programmed cell death in tobacco BY-2 cells. *Planta* **232**: 325–335.

Macek T, Mackova M, Pavlikova D, Szakova J, Truksa M, Singh Cundy A, Kotrba P, Yancey N, Scouten WH. 2002. Accumulation of cadmium by transgenic tobacco. *Acta Biotechnologica* **22**: 101–106.

Mendoza-Cózatl DG, Jobe TO, Hauser F, Schroeder JI. 2011. Long-distance transport, vacuolar sequestration, tolerance, and transcriptional responses induced by cadmium and arsenic. *Current Opinion in Plant Biology* **14**: 554–562.

Mori S, Uraguchi S, Ishikawa S, Arao T. 2009. Xylem loading process is a critical factor in determining Cd accumulation in the shoots of *Solanum melongena* and *Solanum torvum*. *Environmental and Experimental Botany* **67**: 127–132.

Murashige T, Skoog F. 1962. A revised medium for rapid growth and bioassays with tobacco tissue cultures. *Physiologia Plantarum* **15**: 473–497.

Penarrubia L, Andres-Colas N, Moreno J, Puig S. 2010. Regulation of copper transport in *Arabidopsis thaliana*: a biochemical oscillator? *Journal of Biological Inorganic Chemistry* **15**: 29–36.

Piñeros MA, Shaff JE, Kochian LV. 1998. Development, characterization, and application of a cadmium-selective microelectrode for the measurement of cadmium fluxes in roots of *Thlaspi* species and wheat. *Plant Physiology* **116**: 1393–1401.

Plaza S, Tearall KL, Zhao FJ, Buchner P, McGrath SP, Hawkesford MJ. 2007. Expression and functional analysis of metal transporter genes in two contrasting ecotypes of the hyperaccumulator *Thlaspi caerulescens*. *Journal of Experimental Botany* **58**: 1717–1728.

Qu ZL, Zhong NQ, Wang HY, Chen AP, Jian GL, Xia GX. 2006. Ectopic expression of the cotton non-symbiotic hemoglobin gene *GhHbd1* triggers defense responses and increases disease tolerance in *Arabidopsis*. *Plant and Cell Physiology* **47**: 1058–1068.

Reid RJ, Dunbar KR, McLaughlin MJ. 2003. Cadmium loading into potato tubers: the roles of the periderm, xylem and phloem. *Plant, Cell & Environment* **26**: 201–206.

Sakamoto A, Sakurao S, Fukunaga K, Matsubara T, Ueda-Hashimoto M, Tsukamoto S, Takahashi M, Morikawa H. 2004. Three distinct *Arabidopsis* hemoglobins exhibit peroxidase-like activity and differentially mediate nitrite-dependent protein nitration. *FEBS Letters* **572**: 27–32.

Sancenon V, Puig S, Mira H, Thiele DJ, Penarrubia L. 2003. Identification of a copper transporter family in *Arabidopsis thaliana*. *Plant Molecular Biology* **51**: 577–587.

Schutzendubel A, Polle A. 2002. Plant responses to abiotic stresses: heavy metal-induced oxidative stress and protection by mycorrhization. *Journal of Experimental Botany* **53**: 1351–1365.

Siedlecka A, Krupa Z, Samuelsson G, Oquist G, Gardestrom P. 1997. Primary metabolism in *Phaseolus vulgaris* plants under Cd/Fe interaction. *Plant Physiology and Biochemistry* **35**: 951–957.

Siemianowski O, Mills RF, Williams LE, Antosiewicz DM. 2011. Expression of the P1B-type ATPase *AtHMA4* in tobacco modifies Zn and Cd root to shoot partitioning and metal tolerance. *Plant Biotechnology Journal* **9**: 64–74.

Solti Á, Gáspár L, Mészáros I, Szigeti Z, Lévai L, Sárvári É. 2008. Impact of iron supply on the kinetics of recovery of photosynthesis in Cd-stressed poplar (*Populus glauca*). *Annals of Botany* **102**: 771–782.

Stamler JS. 1994. Redox signaling: nitrosylation and related target interactions of nitric oxide. *Cell* **78**: 931–936.

Stamler JS, Lamas S, Fang FC. 2001. Nitrosylation-the prototypic redox-based signaling mechanism. *Cell* **106**: 675–683.

Sun Rl, Zhou QX, Jin CX. 2006. Cadmium accumulation in relation to organic acids in leaves of *Solanum nigrum* L. as a newly found cadmium hyperaccumulator. *Plant and Soil* **285**: 125–134.

Talke IN, Hanikenne M, Kramer U. 2006. Zinc-dependent global transcriptional control, transcriptional deregulation, and higher gene copy number for genes in metal homeostasis of the hyperaccumulator *Arabidopsis halleri*. *Plant Physiology* **142**: 148–167.

Tanaka K, Fujimaki S, Fujiwara T, Yoneyama T, Hayashi H. 2003. Cadmium concentrations in the phloem sap of rice plant (*Oryza sativa* L.) treated with a nutrient solution containing cadmium. *Soil Science and Plant Nutrition* **49**: 311–313.

Thiel J, Rolletschek H, Friedel S, Lunn JE, Nguyen TH, Feil R, Tschiersch H, Müller M, Borisjuk L. 2011. Seed-specific elevation of non-symbiotic hemoglobin AtHb1: beneficial effects and underlying molecular networks in *Arabidopsis thaliana*. *BMC Plant Biology* **11**: 48.

Ueno D, Milner MJ, Yamaji N, Yokosho K, Koyama E, Zambrano MC, Kaskie M, Ebbs S, Kochian LV, Ma JF. 2011. Elevated expression of *TcHMA3* plays a key role in the extreme Cd tolerance in a Cd-hyperaccumulating ecotype of *Thlaspi caerulescens*. *Plant Journal* **66**: 852–862.

Varotto C, Maiwald D, Pesaresi P, Jahns P, Salamini F, Leister D. 2002. The metal ion transporter *IRT1* is necessary for iron homeostasis and efficient photosynthesis in *Arabidopsis thaliana*. *Plant Journal* **31**: 589–599.

Verbruggen N, Hermans C, Schat H. 2009. Molecular mechanisms of metal hyperaccumulation in plants. *New Phytologist* **181**: 759–776.

Verma S, Mishra SN. 2005. Putrescine alleviation of growth in salt stressed *Brassica juncea* by inducing antioxidative defense system. *Journal of Plant Physiology* **162**: 669–677.

Verret F, Gravot A, Auroy P, Leonhardt N, David P, Nussaume L, Vavasseur A, Richaud P. 2004. Overexpression of *AtHMA4* enhances root-to-shoot translocation of zinc and cadmium and plant metal tolerance. *FEBS Letters* **576**: 306–312.

Vert G, Barberon M, Zelazny E, Seguela M, Briat JF, Curie C. 2009. *Arabidopsis IRT2* cooperates with the high-affinity iron uptake system to maintain iron homeostasis in root epidermal cells. *Planta* **229**: 1171–1179.

Vert G, Grotz N, Dedaldechamp F, Gaymard F, Guerinot ML, Briat JF, Curie C. 2002. *IRT1*, an *Arabidopsis* transporter essential for iron uptake from the soil and for plant growth. *The Plant Cell* **14**: 1223–1233.

Wang Z, Zhang YX, Huang ZB, Huang L. 2008. Antioxidative response of metal-accumulator and non-accumulator plants under cadmium stress. *Plant and Soil* **310**: 137–149.

Weber M, Trampczynska A, Clemens S. 2006. Comparative transcriptome analysis of toxic metal responses in *Arabidopsis thaliana* and the Cd^{2+}-hypertolerant facultative metallophyte *Arabidopsis halleri*. *Plant, Cell & Environment* **29**: 950–963.

Wei SH, Zhou QX, Wang X, Cao W, Ren LP, Song YF. 2004. Potential of weed species applied to remediation of soils contaminated with heavy metals. *Journal of Environmental Science (China)* **16**: 868–873.

White PJ, Brown PH. 2010. Plant nutrition for sustainable development and global health. *Annals of Botany* **105**: 1073–1080.

Wintz H, Fox T, Wu YY, Feng V, Chen WQ, Chang HS, Zhu T, Vulpe C. 2003. Expression profiles of *Arabidopsis thaliana* in mineral deficiencies reveal novel transporters involved in metal homeostasis. *Journal of Biological Chemistry* **278**: 47644–47653.

Wong CKE, Cobbett CS. 2009. HMA P-type ATPases are the major mechanism for root-to-shoot Cd translocation in *Arabidopsis thaliana*. *New Phytologist* **181**: 71–78.

Wong CKE, Jarvis RS, Sherson SM, Cobbett CS. 2009. Functional analysis of the heavy metal binding domains of the Zn/Cd-transporting ATPase, *HMA2*, in *Arabidopsis thaliana*. *New Phytologist* **181**: 79–88.

Wu HL, Chen CL, Du J, Liu HF, Yan C, Zhang Y, He YJ, Wang YQ, Chu CC, Feng ZY *et al.* 2012. Co-overexpression *FIT* with *AtbHLH38* or *AtbHLH39* in Arabidopsis enhanced cadmium tolerance *via* increased cadmium sequestration in roots and improved iron homeostasis of shoots. *Plant Physiology* **158**: 790–800.

Xing JP, Jiang RF, Ueno D, Ma JF, Schat H, McGrath SP, Zhao FJ. 2008. Variation in root-to-shoot translocation of cadmium and zinc among different accessions of the hyperaccumulators *Thlaspi* caerulescens and *Thlaspi praecox*. *New Phytologist* **178**: 315–325.

Xu J, Wang WY, Sun JH, Zhang Y, Ge Q, Du LG, Yin HX, Liu XJ. 2011. Involvement of auxin and nitric oxide in plant Cd-stress responses. *Plant and Soil* **346**: 107–119.

Xu J, Yin HX, Li X. 2009. Protective effects of proline against cadmium toxicity in micropropagated hyperaccumulator, *Solanum nigrum* L. *Plant Cell Reports* **28**: 325–333.

Xu J, Yin HX, Li YL, Liu XJ. 2010. Nitric oxide is associated with long-term zinc tolerance in *Solanum nigrum*. *Plant Physiology* **154**: 1319–1334.

Yamaguchi H, Fukuoka H, Arao T, Ohyama A, Nunome T, Miyatake K, Negoro S. 2010. Gene expression analysis in cadmium-stressed roots of a low cadmium-accumulating solanaceous plant, *Solanum torvum*. *Journal of Experimental Botany* **61**: 423–437.

Yoshihara T, Hodoshima H, Miyano Y, Shoji K, Shimada H, Goto F. 2006. Cadmium inducible Fe deficiency responses observed from macro and molecular views in tobacco plants. *Plant Cell Reports* **25**: 365–373.

Supporting Information

Additional supporting information may be found in the online version of this article.

Fig. S1 Sequencing quality evaluation and the distribution of tag expression.

Fig. S2 Gene expression stability and pairwise variation of the candidate reference genes.

Fig. S3 Summary of the experimental process of DGE analysis.

Fig. S4 Procedure for tag preparation.

Fig. S5 Bioinformatics analysis procedure for DGE profiling data.

Tables S1 List of the primers for RT-PCR analysis of the genes

Tables S2 List of differentially expressed genes

Methods S1 Supplemental materials and methods.

Please note: Wiley-Blackwell are not responsible for the content or functionality of any supporting information supplied by the authors. Any queries (other than missing material) should be directed to the *New Phytologist* Central Office.